# Electronic Supplementary Information(ESI)

# Highly Sensitive Ratiometric Fluorescence Probes for Nitric Oxide Based on Dihydropyridine and Potentially Useful in Bioimaging

**Ajit Kumar Mahapatra,[*a] Syed Samim Ali,[a] Kalipada Maiti,[a] Sanchita Mondal,[a] Rajkishor Maji,[a] Srimanta Manna,[a] Saikat Kumar Manna,[a] Md. Raihan Uddin,[b] and Sukhendu Mandal [b]**

[a]Department of Chemistry, Indian Institute of Engineering Science and Technology, Shibpur, Howrah – 711103, India.

[b]Department of Microbiology, Ballygunge Science College, Kolkata- 700019.

*Corresponding author: Tel.: +91 33 2668 4561; fax: +91 33 26684564;

E-mail: mahapatra574@gmail.com

**General Information.**

**Finding the Detection Limit**. The detection limit was calculated on the basis of the fluorescence titration .The fluorescence emission spectrum of **PyNO** and **TPANO** were measured, and the standard deviation of blank measurement was achieved. To gain the slope, the ratio of the fluorescence intensity was plotted as a concentration of NO. So the detection limit was calculated with the following equation.

$$\text{Detection limit} = 3Sb1/S \qquad (1)$$

where Sbl is the standard deviation of blank measurement and S is the slope of the calibration curve.

**Cytotoxicity Assay.** The cytotoxic effects of **TPANO** and [**TPANO** + NO] were determined by MTT assay following the manufacturer's instruction (MTT 2003, Sigma-Aldrich, MO). Vero cells were seeded onto 96-well plates (approximately 104 cells per well) for 24 h. Next day media was removed and various concentrations of probe **TPANO**, NO (0, 0.625,1.25, 2.50 and 5.0 μM) made in DMEM were added to the cells and incubated for 24 h. Solvent control samples (cells treated with DMSO in DMEM), no cells and cells in DMEM without any treatment were also included in the study. Following incubation, the growth media was removed, and fresh DMEM containing MTT solution was added. Subsequently, the supernatant was removed, the insoluble colored formazan product was solubilized in DMSO, and its absorbance was measured in a microtiter plate reader (Perkin-Elmer) at 570. The cell viability was calculated by the following formula: (mean OD in treated wells / mean OD in control wells) x 100.

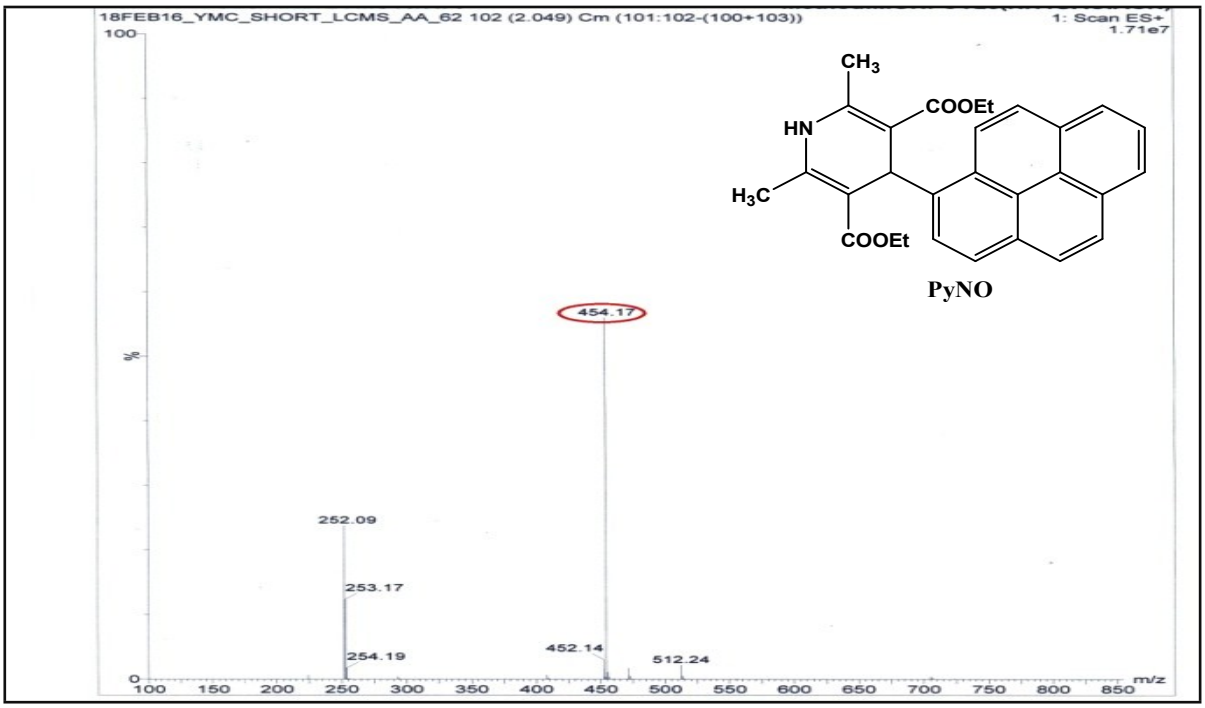


**Figure S1.** LCMS of **PyNO**

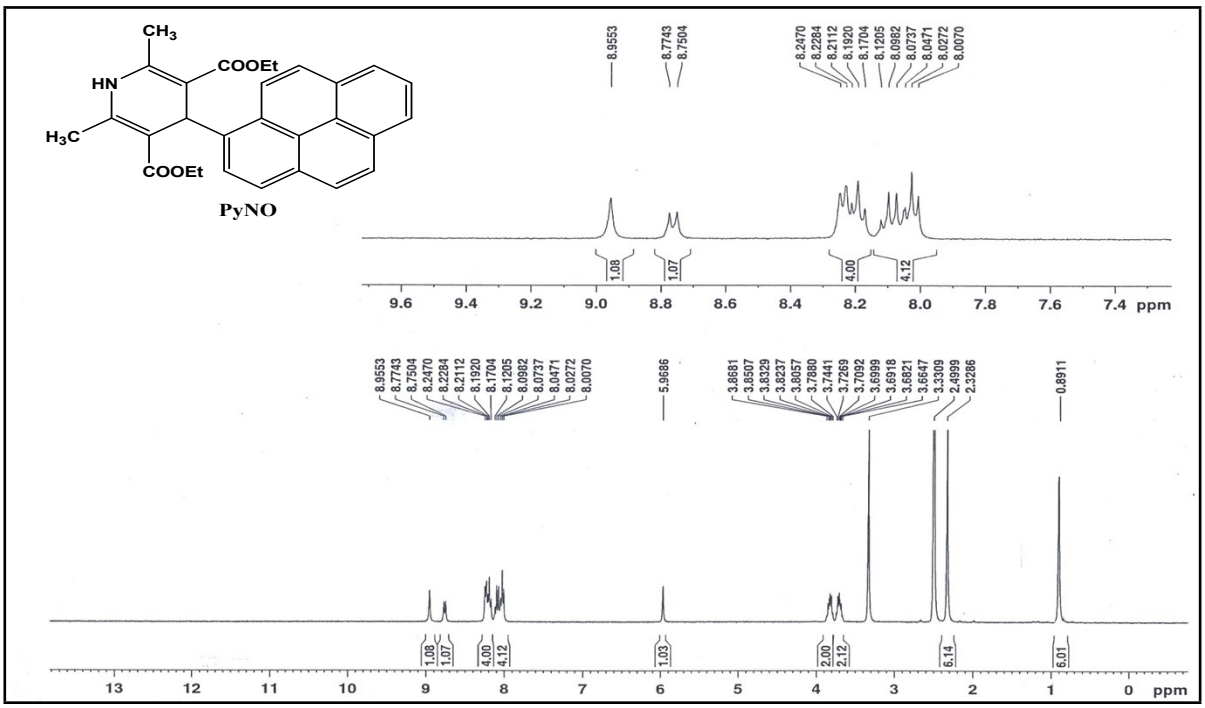


**Figure S2.** $^{1}$H NMR spectra of **PyNO**

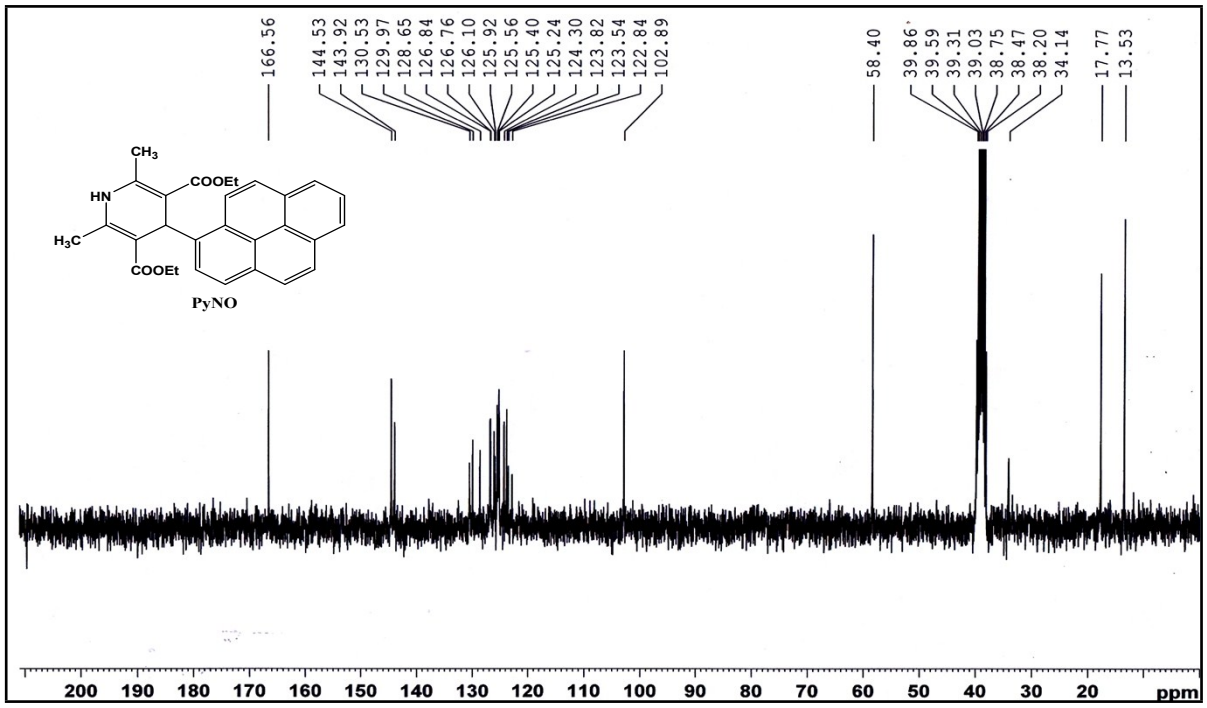


**Figure S3.** $^{13}C$ NMR spectra of **PyNO**

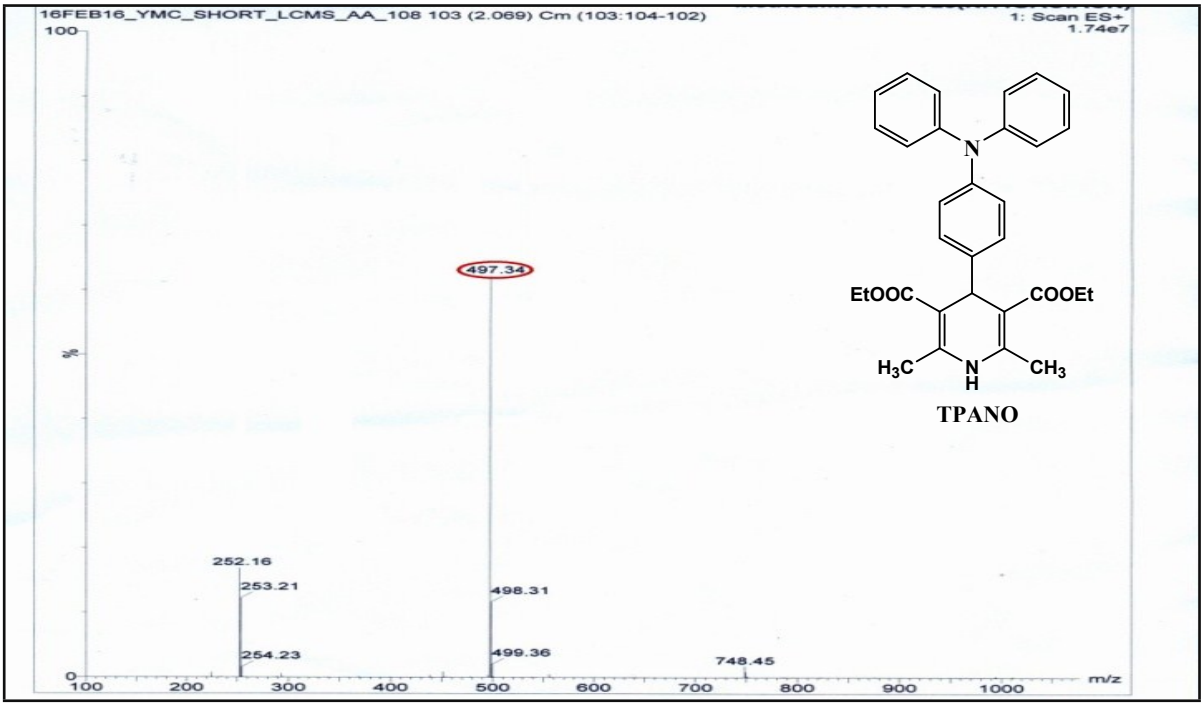


**Figure S4.** LCMS of **TPANO.**

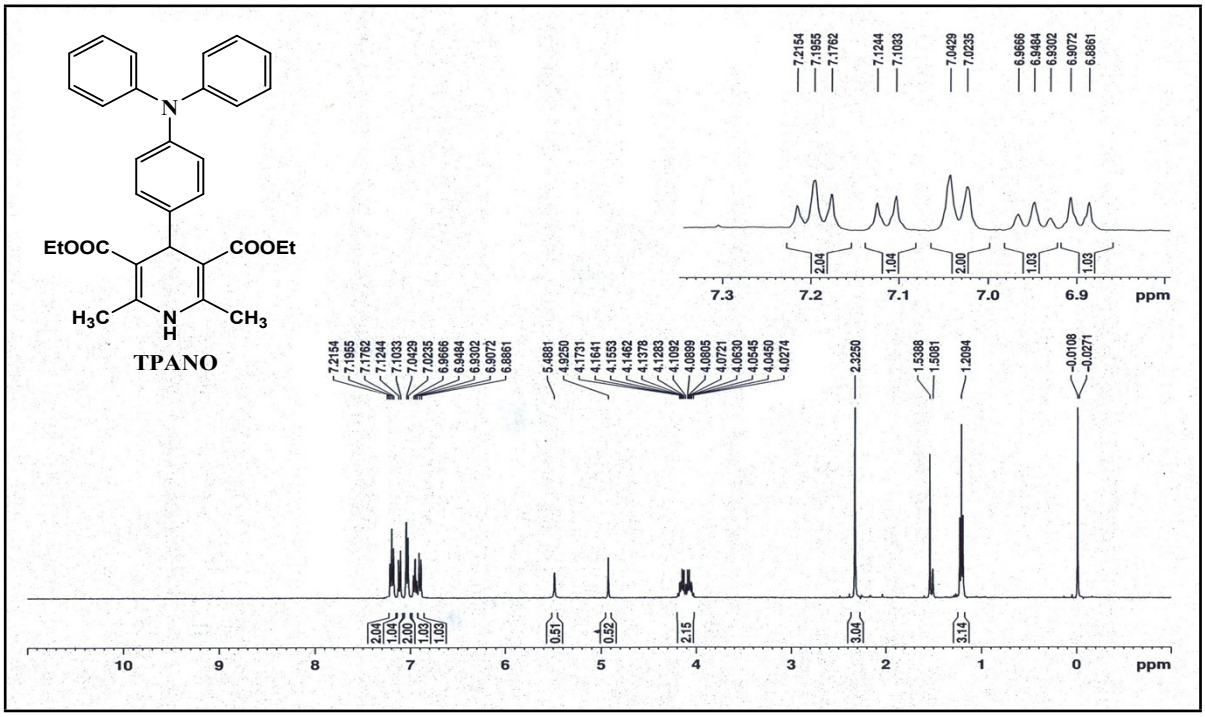


**Figure S5.** $^{1}$H NMR spectra of **TPANO.**

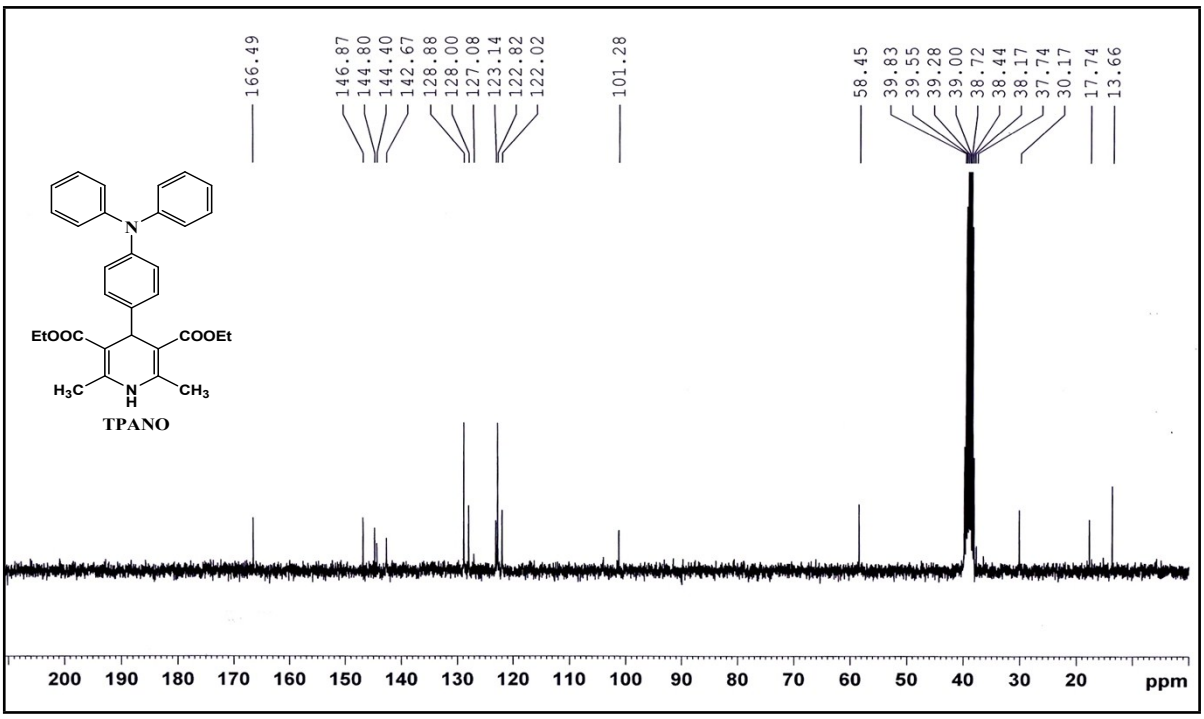


**Figure S6.** $^{13}$C NMR spectra of **TPANO.**

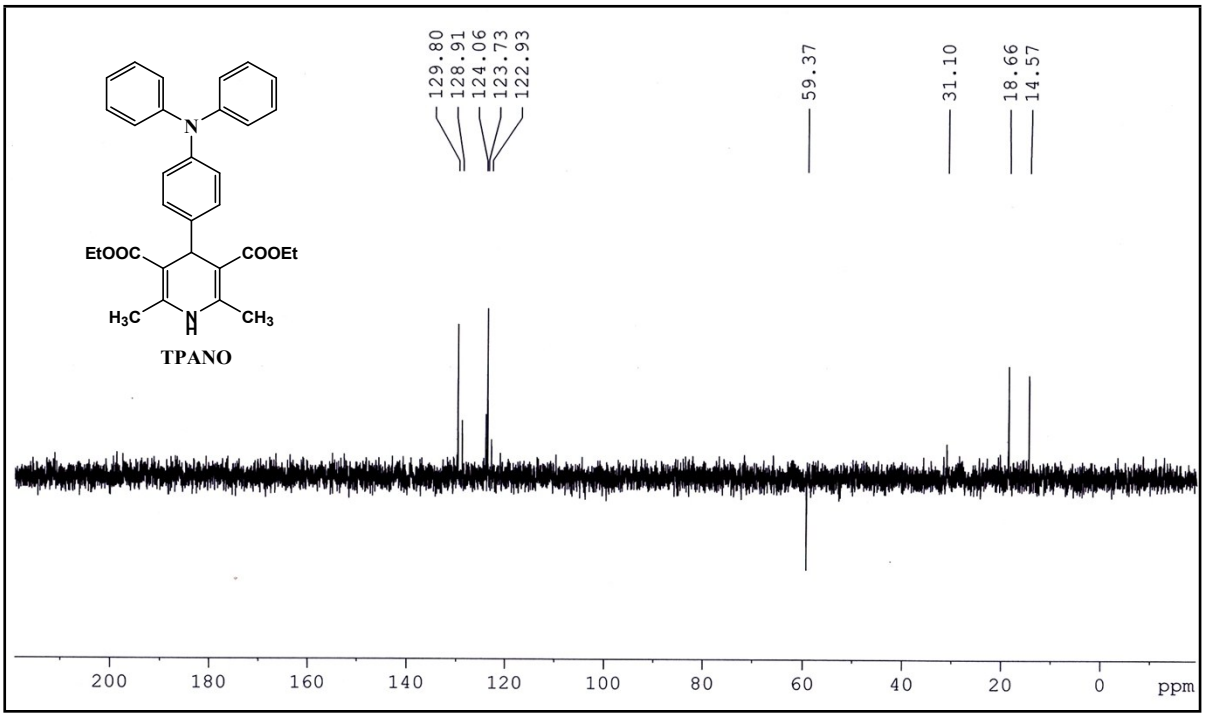


**Figure S7.** DEPT spectra of **TPANO.**

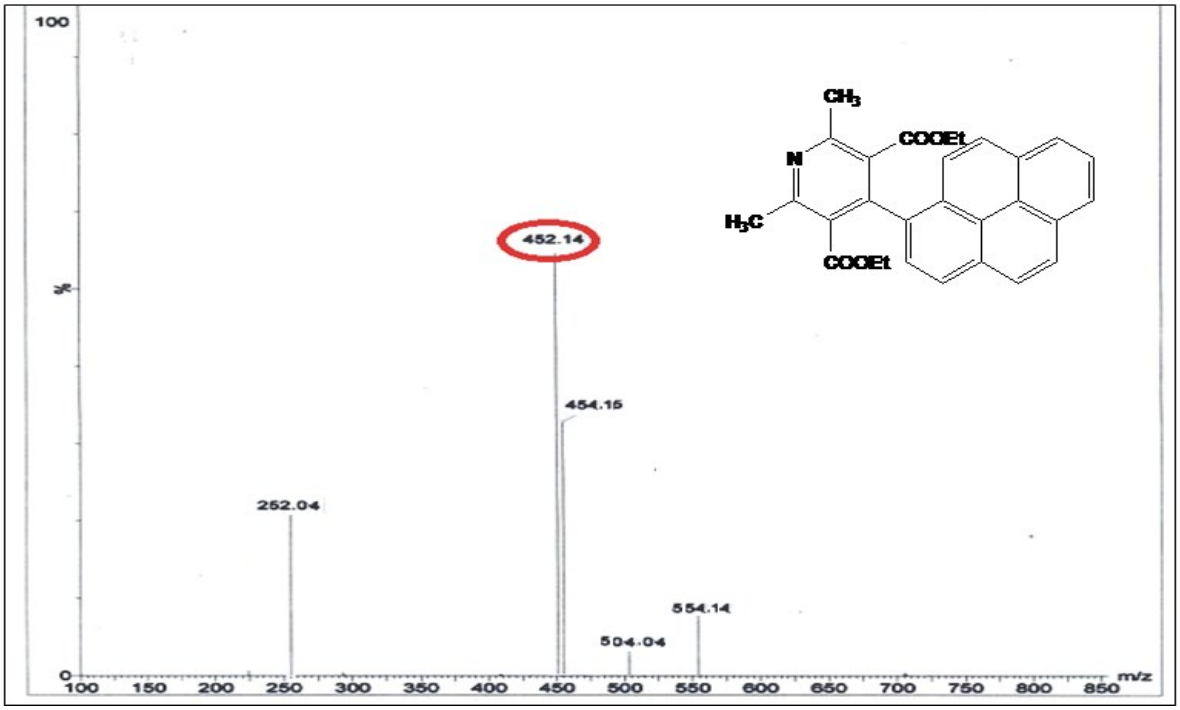


**Figure S8.** LCMS spectra of **PyNO-Ar.**

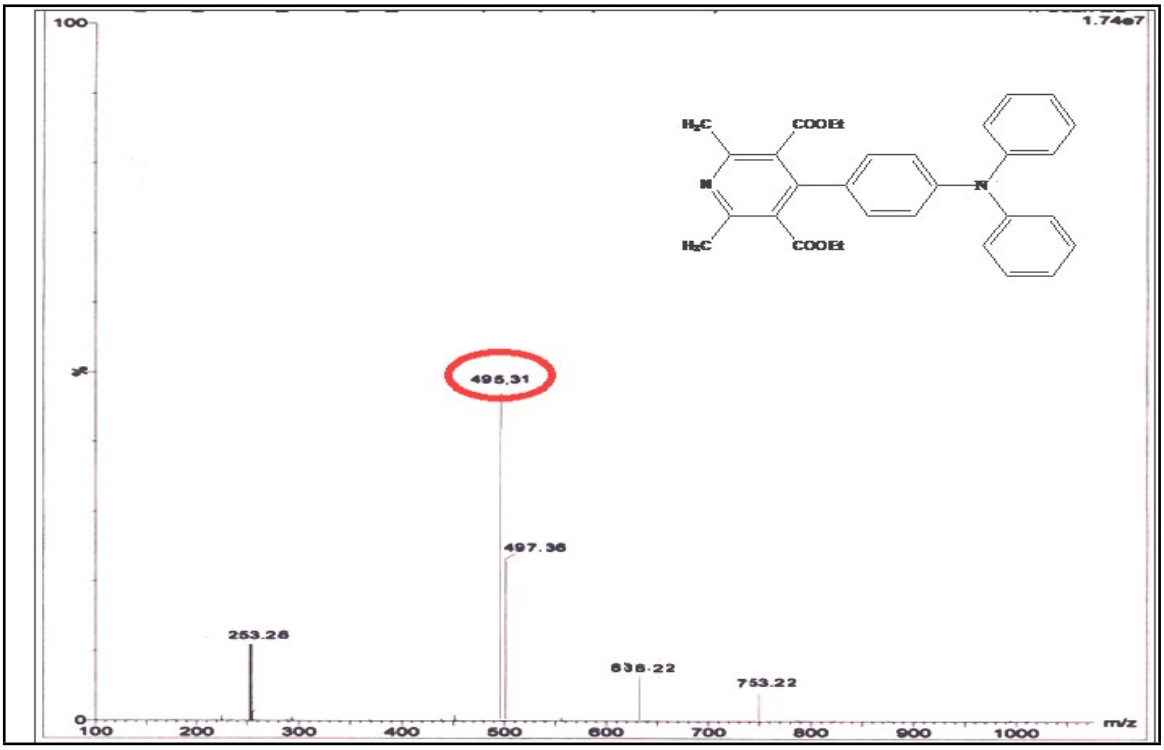


**Figure S9.** LCMS spectra of **TPANO-Ar.**

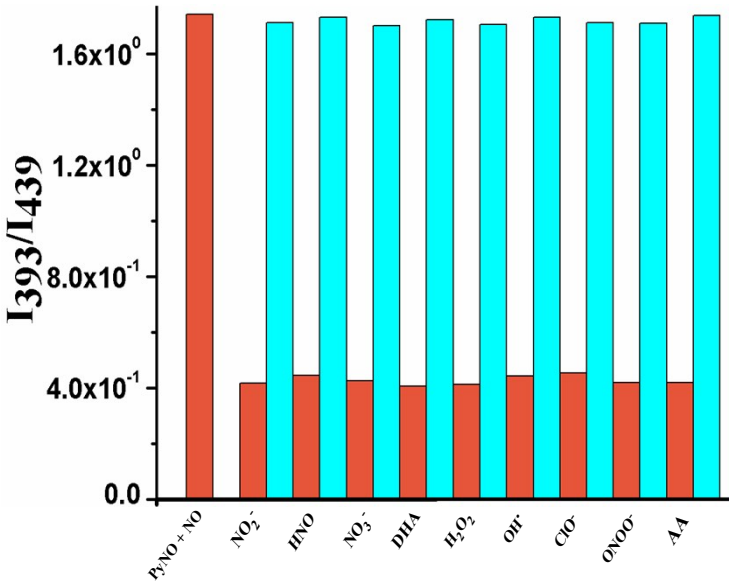


**Figure S10**. Competitive fluorescence response of **PyNO.**

**Quantum yield calculation:**

Here, the quantum yield φ was measured by using the following equation:

$\varphi_x = \varphi_s ( F_x / F_s)( A_s / A_x)(n_x^2/ n_s^2)$

Where,

X & S indicate the unknown and standard solution respectively, φ = quantum yield,

F = area under the emission curve, A = absorbance at the excitation wave length,

n = index of refraction of the solvent. Here φ measurements were performed using Fluorescein in 0.1 M NaOH as standard [φ = 0.79] and Anthracene[φ = 0.36].

For standard (s) Fluorescein in 0.1 M NaOH the following values were determined:

$n_s$ = 1.3330 (for 0.1 M NaOH); $n_x$=1.4793 (for DMSO); φ = 0.79.

For standard (s) Anthracene the following values were determined:

$n_s$ = 1.4793; $n_x$=1.4793 (for DMSO); φ = 0.36.

Using the above equation, we calculated quantum yield of probes .

| **Probes** | **Quantum yield** (φ) |
|---|---|
| **TPANO** | 0.02 |
| **TPANO-Ar** | 0.51 |
| **PyNO** | 0.15 |
| **PyNO-Ar** | 0.31 |

**Table S1.** Quantum yield data

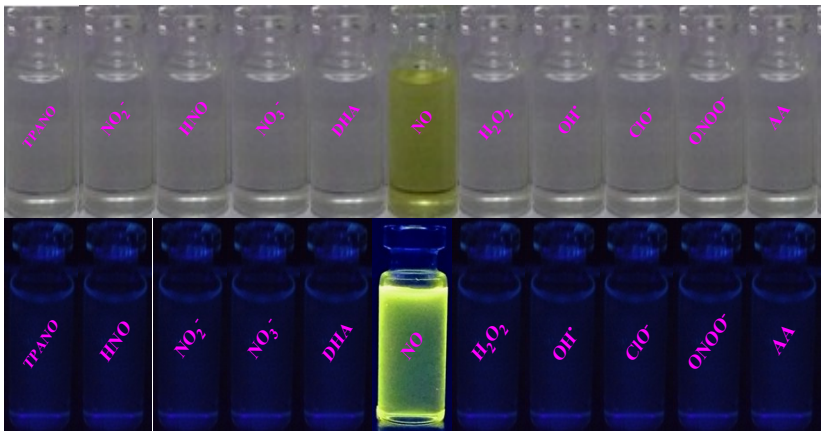


**Figure S11.** The visible color (top) and fluorescence changes (buttom) of receptor **TPANO** in aq. DMSO (DMSO: $H_2O$ = 7:3 v/v, 20 mM HEPES buffer, pH = 7.4) upon addition of various ions.

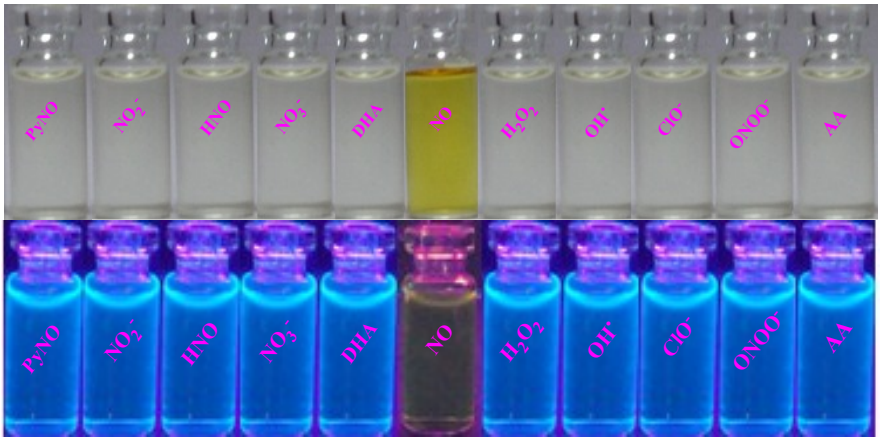


**Figure S12.** The visible color (top) and fluorescence changes (buttom) of receptor **PyNO** in aq. DMSO (DMSO: $H_2O$ = 7:3 v/v, 20 mM HEPES buffer, pH = 7.4) upon addition of various ions.

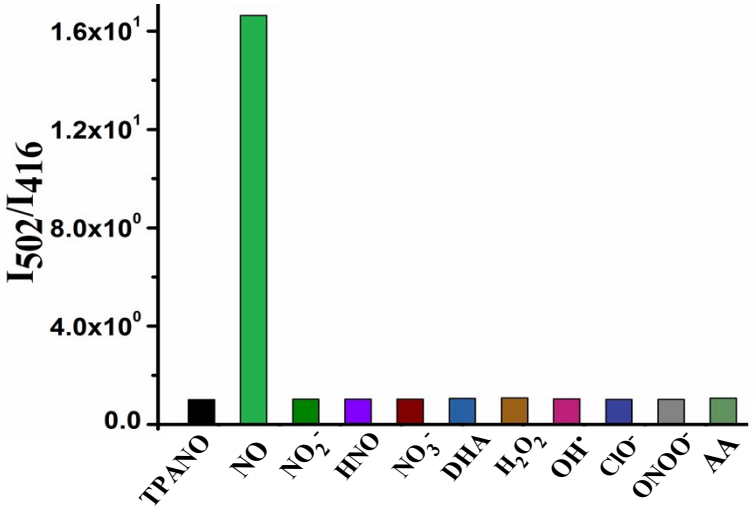


**Figure S13.** Bar profiles of fluorescence changes of **TPANO** and in presence of other ions.

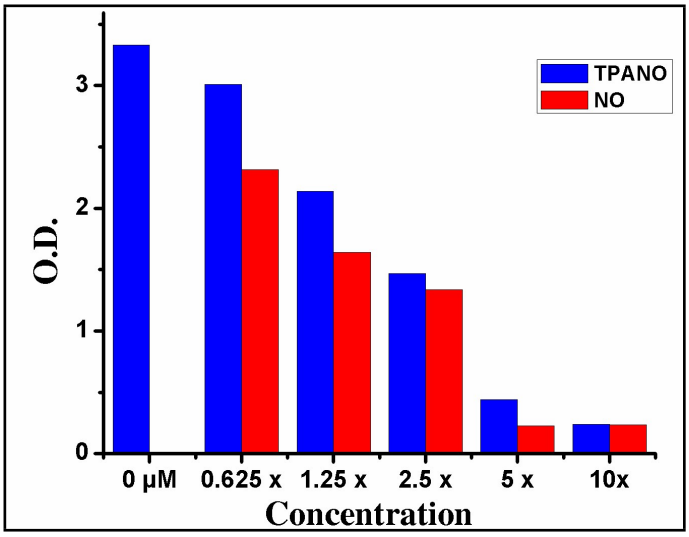


**Figure S14.** MTT assay to determine the cytotoxic effect of **TPANO** on Vero cell .

**Computational Method:**

Geometries have been optimized in B3LYP density functional method with 6-31+G (d, p) basis set for all atom. The geometries are verified as proper minima or not by frequency calculations.

Time-dependent density functional theory calculation has also been performed at the same level of theory.

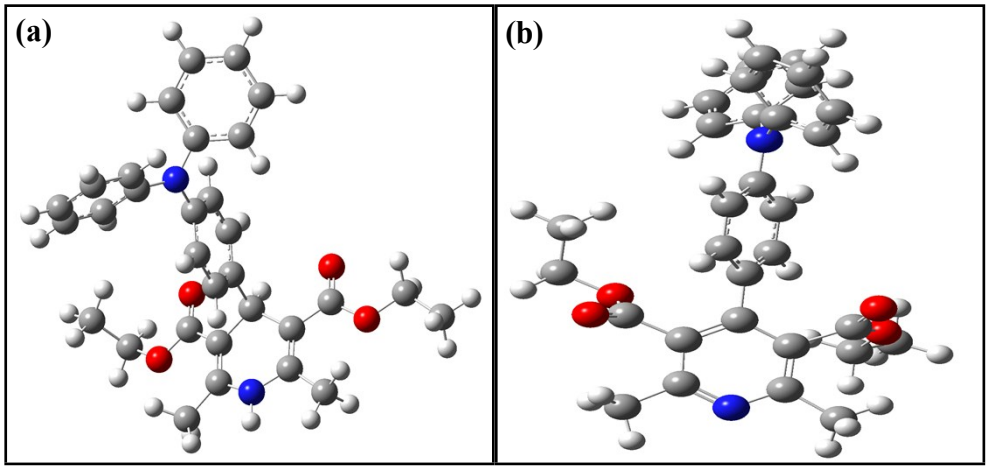


**Figure S15.** Energy minimization structure of (a) **TPANO** and (b) **TPANO-Ar.**

| Species | E(HOMO) | E(LUMO) | E(LUMO+2) | E(LUMO+3) | E(LUMO+4) |
|---|---|---|---|---|---|
| **TPANO** | 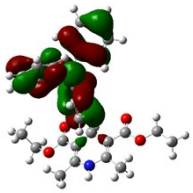 **(-3.45 eV)** | 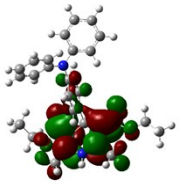 **(-1.12 eV)** | 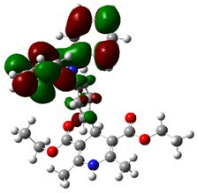 **(0.25 eV)** | 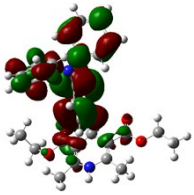 **(+0.65 eV)** | 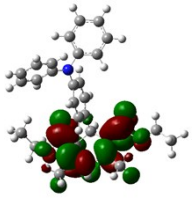 **(+1.02 eV)** |
| **TPANO-Ar** | 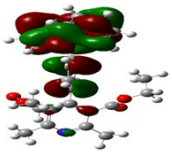 **(-6.91 eV)** | 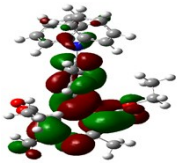 **(5.10 eV)** | 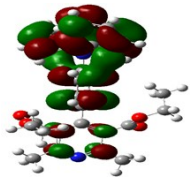 **(-1.70 eV)** | 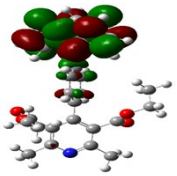 **(+1.82 eV)** | 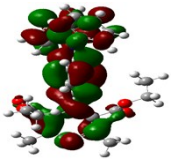 **(+2.70 eV)** |

**Table S2**. HOMO-LUMO energy calculated data of **TPANO** and **TPANO-Ar.**

| $\lambda_{max}$(nm) | Osc. Strength (*f*) | Key Excitations |
|---|---|---|
| 307.63 | 0.3139 | (96.55%)HOMO→LUMO+2 |
| 300.37 | 0.3043 | (96.71%)HOMO→LUMO+3 |

**Table S3**. Selected vertical electronic transitions of **TPANO** calculated by TDDFT method.

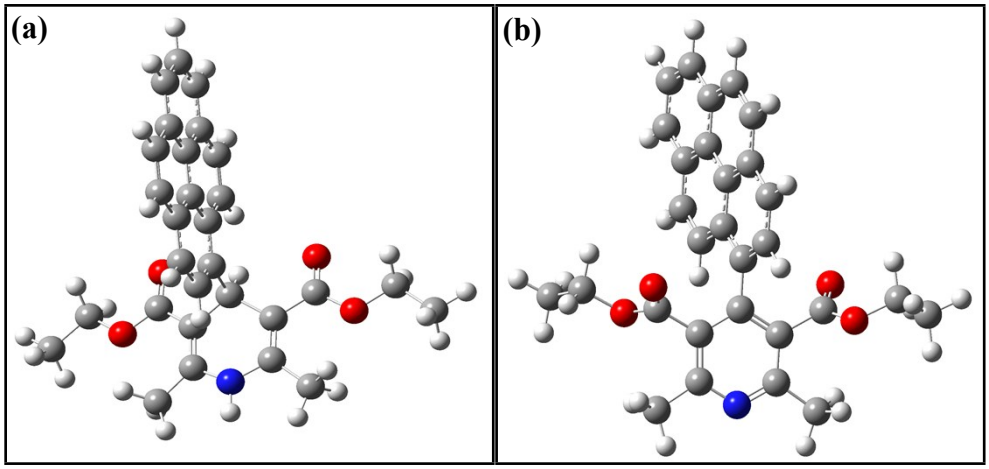


**Figure S16.** Energy minimization structure of (a) **PyNO** and (b) **PyNO-Ar.**

| $\lambda_{max}$(nm) | Osc. Strength (*f*) | Key Excitations |
|---|---|---|
| 323.34 | 0.1138 | (82.07%)HOMO→LUMO+1 |
| 320.73 | 0.1776 | (98.36%)HOMO-1→ LUMO+1 |

**Table S4.** Selected vertical electronic transitions of **PyNO** calculated by TDDFT method.

| Species | E(HOMO) | E(LUMO) | E(HOMO-1) | E(LUMO+1) | E(LUMO+2) |
|---|---|---|---|---|---|
| PyNO | 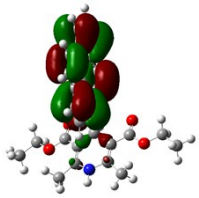 (-3.75 eV) | 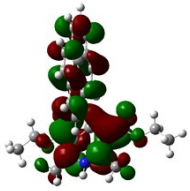 (-1.16 eV) | 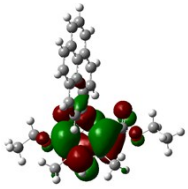 (-5.13 eV) | 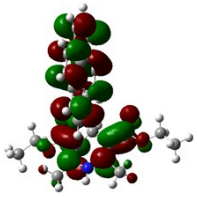 (-0.85 eV) | 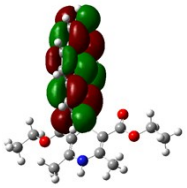 (-0.43 eV) |
| PyNO-Ar | 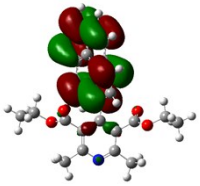 (-5.32 eV) | 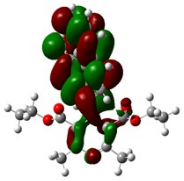 (-1.60 eV) | 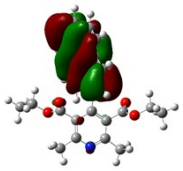 (-6.22 eV) | 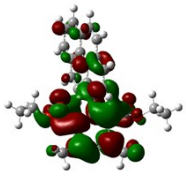 (-1.04 eV) | 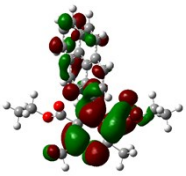 (-0.78 eV) |

**Table S5**. HOMO-LUMO energy calculated data of **PyNO** and **PyNO-Ar.**

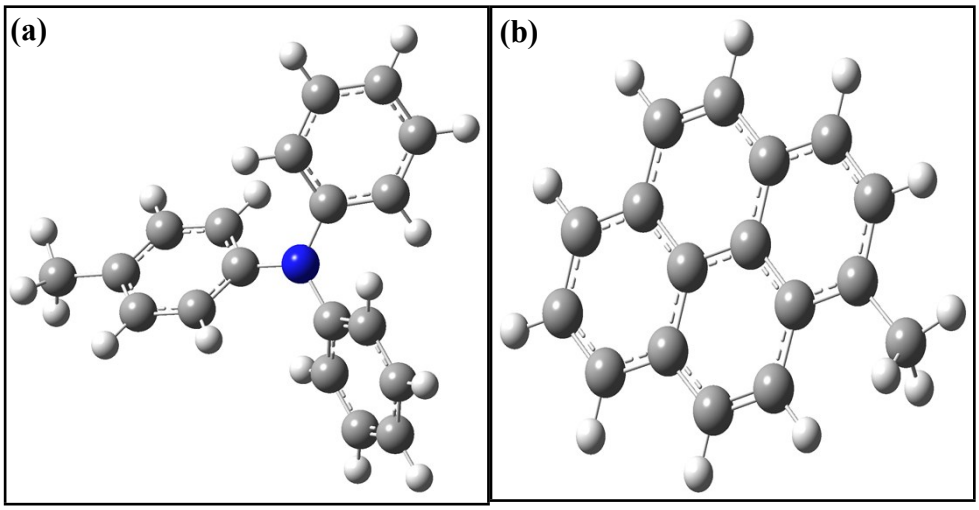


**Figure S17.** Energy minimization structure of (a) **TPANO-Me** and (b) **PyNO-Me.**

| Species | E(HOMO) | E(LUMO) |
|---|---|---|
| TPANO-Me | 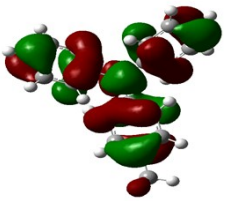 (-4.88 eV) | 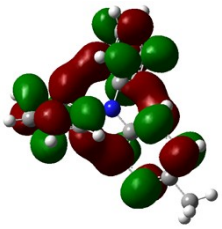 (-2.92 eV) |
| PyNO-Me | 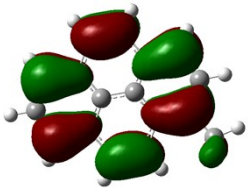 (-3.11 eV) | 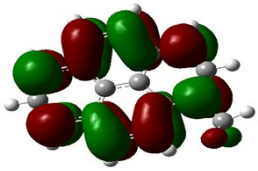 (-0.94 eV) |

**Table S6**. HOMO-LUMO energy calculated data of **TPANO-Me** and **PyNO-Me.**

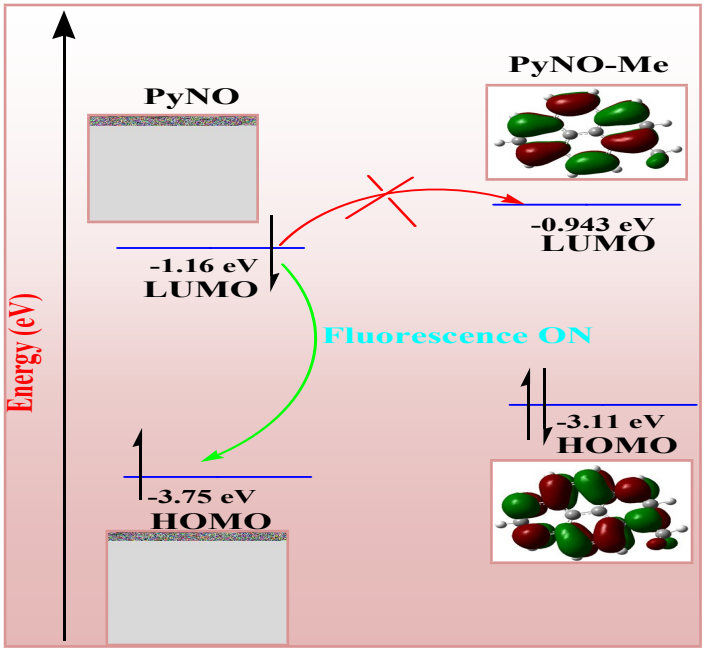


**Figure S18.** Calculated energy level diagram of **PyNO** and **PyNO-Me.**

**Table S7**. Crystal Data and Details of the Structure Determination for **TPANO** and **PyNO**

| **Compound** | **TPANO** | **PyNO** |
|---|---|---|
| CCDC Entry | 1499388 | 1499389 |
| Formula | $C_{31}$ $H_{32}$ $N_2$ $O_4$ | $C_{29}$ $H_{22}$ N $O_4$ |
| Formula Weight | 496.58 | 448.13 |
| Crystal Color | green | yellow |
| Crystal System | Monoclinic | Monoclinic |
| Space group | P21/n | P21 |
| a, b, c (Å) | 11.9094(13), 7.3443(8), 30.494(4) | 8.690(5), 9.930(5), 13.591(5) |
| α(°) | 90.00 | 90.000(5) |
| β(°) | 91.547(4) | 90.853(5) |
| γ(°) | 90.00 | 90.000(5) |
| V(Å$^3$) | 2666.2(5) | 1172.7(10) |
| Z | 4 | 2 |
| D(calculated) [g/cm$^3$] | 1.237 | 1.270 |
| Mu(MoKa) [mm$^{-1}$] | 0.082 | 0.085 |
| F(000) | 1056 | 470 |
| Crystal Size [mm] | 0.30× 0.22×0.16 | 0.20× 0.12×0.10 |
| Absorption Correction | Multi-scan | Multi-scan |
| Temperature (K) | 295(2) | 293(2) |

| | | |
|---|---|---|
| Radiation [Å] | 0.71073 | 0.71073 |
| θ(Min-Max) [$^0$] | 2.60– 28.28 | 2.3–28.3 |
| Dataset (h; k; l) | -15 to 15; - 9 to 9; -40 to 40 | -11 to 11; - 13 to 13; -18 to 18 |
| Total, Unique Data, R(int) | 37027, 5365,0.0877 | 22479, 4735,0.1134 |
| Observed data [I > 2σ(I)] | 5365 | 4735 |
| Nref, Npar | 6656, 351 | 5847, 316 |
| R, wR, S | 0.1066, 0.2118, 1.028 | 0.0867, 0.2181, 1.047 |
| Δq(max)and Δq(min) (e/Å$^3$) | 0.44 and -0.33 | 0.365 and -0.258 |
| Goodness of Fits | 1.028 | 1.047 |

$R = \sum |(|F_o| - |F_c|)| / \sum |F_o|$

$wR = \{\sum [w(F_o^2 - F_c^2)^2] / \sum [w(F_o^2)^2]\}^{1/2}$

$w = 1/[\sigma^2(F_o^2) + (0.0721P)^2 + 2.3397P]$ for **TPANO**

$w = 1/[\sigma^2(F_o^2) + (0.1015P)^2 + 0.3581P]$ for **PyNO**

Where$P = (F_c^2 + 2F_c^2)/3$.

*GOF (S)* $= \{\sum [w(F_o^2 - F_c^2)^2]/(n-p)\}^{1/2}$, where $n$ = number of measured data and $p$ = number of parameters.

**Table S8.** Selected bond distances (Å) and bond angles (°) of **TPANO** and **PyNO**

| **TPANO** | | | **PyNO** | | |
|---|---|---|---|---|---|
| Bonds(Å) | X-ray | DFT data | Bonds(Å) | X-ray | DFT data |
| O1 – C25 | 1.202(3) | 1.2202 | C1 – C17 | 1.529(6) | 1.5399 |
| O2 – C25 | 1.335(3) | 1.3642 | C17 – C18 | 1.531(6) | 1.5270 |
| O3 – C29 | 1.195(3) | 1.2198 | C17 – C21 | 1.515(7) | 1.5271 |
| O4 – C29 | 1.380(9) | 1.3632 | N1 – C19 | 1.381(6) | 1.3895 |
| N2 – H3A | 0.8600 | 1.0079 | N1 – C20 | 1.366(7) | 1.3895 |
| N2 – C21 | 1.370(3) | 1.3899 | O1 – C22 | 1.192(9) | 1.2199 |
| N2 – C22 | 1.384(3) | 1.3895 | O3 – C25 | 1.206(7) | 1.2199 |
| C19 – H19 | 0.980 | 1.0915 | O2 – C22 | 1.331(7) | 1.3619 |
| C16 – C19 | 1.522(3) | 1.5326 | O4 – C25 | 1.333(6) | 1.3619 |
| **Angles ($^0$)** | | | O2 – C23 | 1.432(7) | 1.4445 |
| C16 – C19 – C20 | 111.6(2) | 111.76 | O4 – C26 | 1.444(7) | 1.4445 |
| C16 – C19 – C23 | 109.0(2) | 111.77 | C26 – C27 | 1.474(13) | 1.5168 |
| C20 – C19 – C23 | 110.2(2) | 111.12 | **Angles ($^0$)** | | |
| C21 – N2 – C22 | 123.1(2) | 124.28 | C18 – C17 – C21 | 110.1(2) | 111.13 |
| | | | C17 – C21 – C20 | 120.7(3) | 120.767 |
| | | | C17 – C18 – C19 | 120.8(2 | 120.767 |
| | | | C18 – C19 – N1 | 119.2(3) | 118.514 |

| | | | | | |
|---|---|---|---|---|---|
| | | | C19 – N1 – C20 | 123.1(3) | 124.27 |

**Table S9.** Analysis of the Hydrogen Bonding Network

| ***TPANO*** | | | | | |
|---|---|---|---|---|---|
| Donor(D) --- H …Acceptor (A) | d $_{N–H}$(Å) | d $_{H---O}$(Å) | d $_{N---O}$(Å) | < (D – H …A)($^{0}$) | symmetry |
| N2—H3A…..O3 | 0.8600 | 2.1400 | 2.996(2) | 175.00 | x, 1+y, z |
| ***PyNO*** | | | | | |
| N1—H1…..O3 | 0.86(4) | 2.16(4) | 2.997(4) | 165(4) | 1-x,-1/2+y,2-z |

Crystallographic data for the structures reported in this paper in the form of CIF files have been deposited with the Cambridge Crystallographic Data Center as supplementary publication Nos. 1499388-1499389 for compound **TPANO** and **PyNO** respectively. Copies of the data can be obtained free of charge via **http://www.ccdc.cam.ac.uk/conts/retrieving.html** or from CCDC, 12 Union Road, Cambridge CB2 IEZ, UK (Fax: + 44 1223 336 033; E-mail: deposit@ccdc.cam.ac.uk).

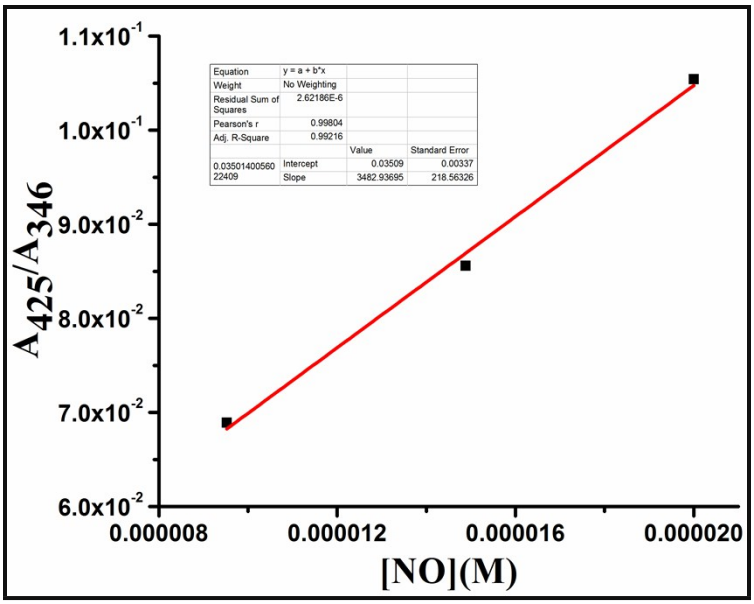


**Figure S19.** Calibration curve for **PyNO** with **NO** by UV-Vis titration.

Thus using the formula we get the detection limit= 2.9 μM.

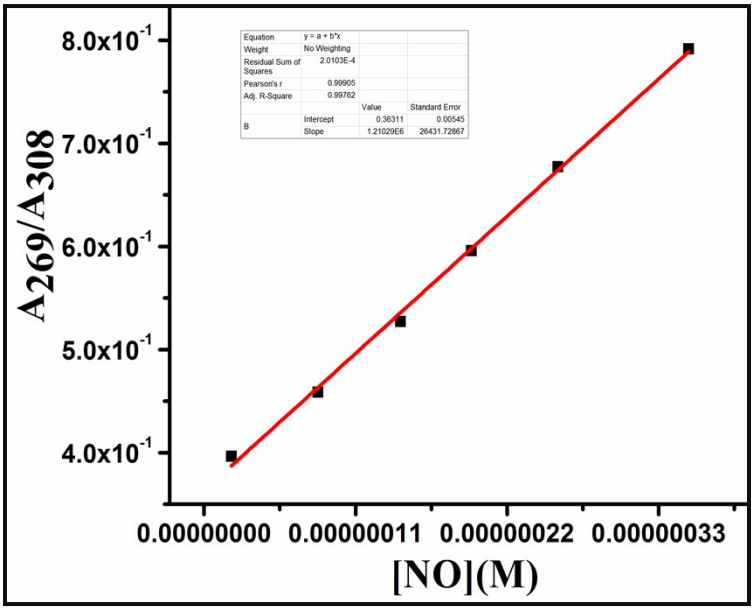


**Figure S20.** Calibration curve for **TPANO** with **NO** by UV-Vis titration.

Thus using the formula we get the detection limit= 0.013 μM.

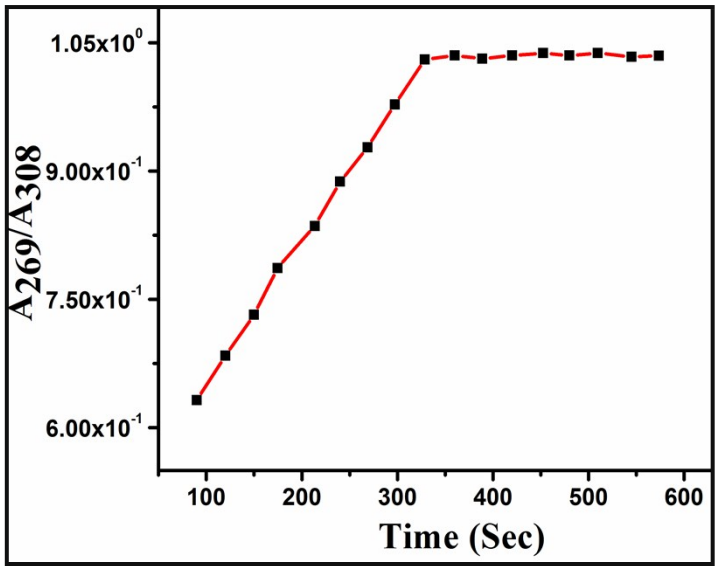


**Figure S21.** Increments of absorption intensity of **TPANO** in pH 7.4,10 mM HEPES buffer against time (0 - 6 min) after the addition of NO at different concentration.

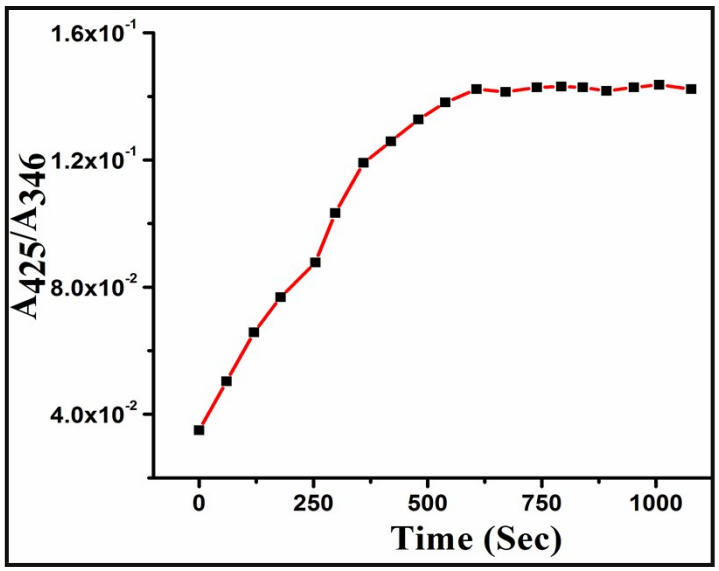


**Figure S22.** Increments of absorption intensity of **PyNO** in pH 7.4,10 mM HEPES buffer against time (0 - 11min) after the addition of NO at different concentration.

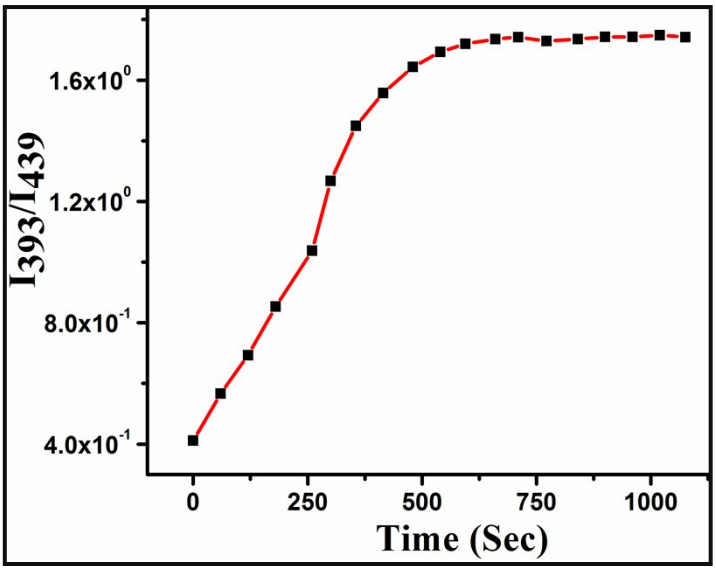


**Figure S23.** Increments of fluorescence intensity of **PyNO** in pH 7.4,10 mM HEPES buffer against time (0 - 11min) after the addition of NO at different concentration.